3

Low Cost Solar Cells Based on Cuprous Oxide

Verka Georgieva, Atanas Tanusevski[1] and Marina Georgieva
Faculty of Electrical Engineering and Information Technology,
[1]Institute of Physics, Faculty of Natural Sciences and Mathematics,
The "St. Cyril & Methodius" University, Skopje,
R. of Macedonia

1. Introduction

The worldwide quest for clean and renewable energy sources has encouraged large research activities and developments in the field of solar cells. In recent years, considerable attention has been devoted to the development of low cost energy converting devices. One of the most interesting products of photoelectric researches is the semiconductor cuprous oxide cell. As a solar cell material, cuprous oxide -Cu_2O, has the advantages of low cost and great availability. The potential for Cu_2O using in semiconducting devices has been recognized since, at least, 1920. Interest in Cu_2O revived during the mid seventies in the photovoltaic community (Olsen et al.,1982). Several primary characteristics of Cu_2O make it potential material for use in thin film solar cells: its non-toxic nature, a theoretical solar efficiency of about 9-11%, an abundance of copper and the simple and inexpensive process for semiconductor layer formation. Therefore, it is one of the most inexpensive and available semiconductor materials for solar cells. In addition to everything else, cuprous oxide has a band gap of 2.0 eV which is within the acceptable range for solar energy conversion, because all semiconductors with band gap between 1 eV and 2 eV are favorable material for photovoltaic cells (Rai, 1988).

A variety of techniques exist for preparing Cu_2O films on copper or other conducting substrates such as thermal, anodic and chemical oxidation and reactive sputtering. Particularly attractive, however, is the electrodeposition method because of its economy and simplicity for deposition either on metal substrates or on transparent conducting glass slides coated with highly conducting semiconductors, such as indium tin oxide (ITO), SnO_2, In_2O_3 etc. This offers the possibility of making back wall or front wall cells as well. We have to note that electrochemical preparation of cuprous oxide (Cu_2O) thin films has reached considerable attention during the last years.

Electrodeposition method of Cu_2O was first developed by Stareck (Stareck, 1937). It has been described by Rakhshani (Jayanetti & Dharmadasa, 1996, Mukhopadhyay et al.,1992, Rakhshani et al.1987, Rakhshani et al., 1996). In this work, a method of simple processes of electrolysis has been applied.

Electrochemical deposition technique is an simple, versatile and convenient method for producing large area devices. Low temperature growth and the possibility to control film thickness, morphology and composition by readily adjusting the electrical parameters, as well as the composition of the electrolytic solution, make it more attractive. At present,

electrodeposition of binary semiconductors, especially thin films of the family of wide - bend gap II-IV semiconductors (as is ZnO), from aqueous solutions is employed in the preparation of solar cells. A photovoltaic device composed of a p-type semiconducting cuprous (I) oxide (Cu_2O) and n-type zinc oxide (ZnO) has attracted increasing attention as a future thin film solar cell, due to a theoretical conversion efficiency of around 18% and an absorption coefficient higher than that of a Si single crystal (Izaki et al. 2007)
Therefore, thin films of cuprous oxide (Cu_2O) have been made using electrochemical deposition technique. Cuprous oxide was electrodeposited on copper substrates and onto conducting glass coated with tin oxide (SnO_2), indium tin oxide (ITO) and zinc oxide (ZnO). Optimal conditions for high quality of the films were requested and determined. The qualitative structure of electrodeposited thin films was studied by x-ray diffraction (XRD) analysis. Their surface morphology was analyzed with scanning electronic microscope (SEM). The optical band gap values Eg were determined. To complete the systems Cu/Cu_2O, SnO_2/Cu_2O, ITO/Cu_2O and ZnO/Cu_2O as solar cells an electrode of graphite or silver paste was painted on the rear of the Cu_2O. Also a thin layer of nickel was vacuum evaporated on the oxide layer. The parameters of the solar cells, such the open circuit voltage (V_{oc}), the short circuit current (I_{sc}), the fill factor (*FF*), the diode quality factor (*n*), serial (*Rs*) and shunt resistant (*Rsh*) and efficiency (η) were determined. The barrier height (*Vb*) was determined from capacity-voltage characteristics.
Generally is accepted that the efficiency of the cells cannot be much improved. (Minami et al.,2004). But we successed to improve the stability of the cells, using thin layer of ZnO, making heterojunctions Cu_2O based cells.

2. Structural, morphological and optical properties of electrodeposited films of cuprous oxide

2.1 Experimental

2.1.1 Preparation of the films

A very simple apparatus was used for electrodeposition. It is consisted of a thermostat, a glass with solution, two electrodes (cathode and anode) and a standard electrical circuit for electrolysis. The deposition solution contained 64 g/l anhydrous cupric sulphate ($CuSO_4$), 200 ml/l lactic acid ($C_3H_6O_3$) and about 125 g/l sodium hydroxide (NaOH), (Rakhshani et al.1987, Rakhshani & Varghese, 1987). Cupric sulphate was dissolved first in distilled water giving it a light blue color. Then lactic acid was added. Finally, a sodium hydroxide solution was added, changing the color of the solution to dark blue with pH = 9. A copper clad for printed circuit board, with dimension 50 μm, 2.5 × 7 cm^2, was used as the anode. Copper clad and conducting glass slides coated with ITO and SnO_2 were used as a cathode. Experience shows that impurities (such as dirt, finger prints, etc.) on the starting surface material have a significant impact on the quality of the cuprous oxide. Therefore, mechanical and chemical cleaning of the electrodes, prior to the cell preparation, is essential.
Copper boards were polished with fine emery paper. After that, they were washed by liquid detergent and distilled water. The ITO substrates were washed by liquid detergent and rinsed with distilled water. The SnO_2 substrates were soaked in chromsulphuric acid for a few hours and rinsed with distilled water. Before using all of them were dried.
Thin films of Cu_2O were electrodeposited by cathodic reduction of an alkaline cupric lactate solution at 60^0 C . The deposition was carried out in the constant current density regime. The deposition parameters, as current density, voltage between the electrodes and deposition

time were changed. The Cu_2O films were obtained under following conditions: 1) current density j = 1,26 mA/cm², voltage between the electrodes V = 0,3 - 0,38 V and deposition time t = 55 min. Close to the value of current density, deposition time and Faraday's law, the Cu_2O oxide layer thickness was estimated to be about 5 μm.
The potentiostatic mode was used for deposition the Cu_2O films on glass coated with SnO_2 prepared by spray pyrolisis method of 0.1 M water solution of $SnCl_2$ complexes by NH_4F . The applied potential difference between anode and cathode was constant. It was found that suitable value is V = 0,5 to 0,6 V. The deposition current density at the beginning was dependent on the surface resistance of the cathode. For a fixed value of the potential, the current decreased with increasing film thickness. The film thickness was dependent on deposition current density j. For current density of about 1 mA/cm² at the beginning and deposition time of about 2 h, the film thickness was 5-6 μm approximately. The thickness of deposited film was determined using a weighting method, as $d = m/\rho s$, where m is the mass and s is the surface of the film. A density ρ, of 5.9 g/cm³ was used.
The deposition of Cu_2O on a commercial glass coated with ITO was carried out under constant current density. The ITO/Cu_2O films was obtained under the following conditions: current density j = 0,57 mA/cm², voltage between the electrodes V = 1,1 - 1,05 V and deposition time t = 135 min. The Cu_2O oxide layer thickness was estimated to be about 5 μm. All deposited films had reddish to reddish-gray color.

2.1.2 Structural properties

The structure of the films was studied by X – ray diffraction, using CuKα radiation with a wavelength of 0.154 nm. The Bragg angle of 2θ was varied between 20^0 and 50^0. The XRD spectrums of the films samples, deposited on copper, glass coated by SnO_2 and glass coated by ITO are shown in Fig.1, Fig.2 and Fig.3 respectively. It was found that all films are polycrystalline and chemically pure Cu_2O with no traces of CuO. XRD peaks corresponded to Cu_2O and the substrate material. The XRD spectrums indicate a strong Cu_2O peak with (200) preferential orientation.

2.1.3 Morphological properties

The surface morphology of the films was studied by a scanning electron microscope JEOL model JSM 35 CF. Fig.4, Fig.5 and Fig.6 show the scanning electron micrographs of Cu_2O films deposited on copper, glass coated by SnO_2 and glass coated by ITO respectively. The photographs indicate a polycrystalline structure. The grains are very similar to each other in size and in shape. They are about 1 μm and less in size for the film deposited on copper, 1-2 μm for the film deposited on SnO_2 and about 1 μm for the film deposited on ITO.

2.1.4 Optical band-gap energy determination

The optical band-gap is an essential parameter for semiconductor material, especially in photovoltaic conversion. In this work it was determined using the transmittance spectrums of the films. The optical transmission spectrums were recording on Hewlett-Packard (model 8452 A) spectrophotometer in the spectral range 350-800 nm wavelength. Thin layers of a transparent Cu_2O were preparing for the optical transmission spectrums recording. The optical transmission spectrum of about 1,5 μm thick Cu_2O film deposited on glass coated with SnO_2 is presented in Fig.7. There are two curves, one (1) recorded before annealing and the other one (2) after annealing of the film for 3h at 130^0C.

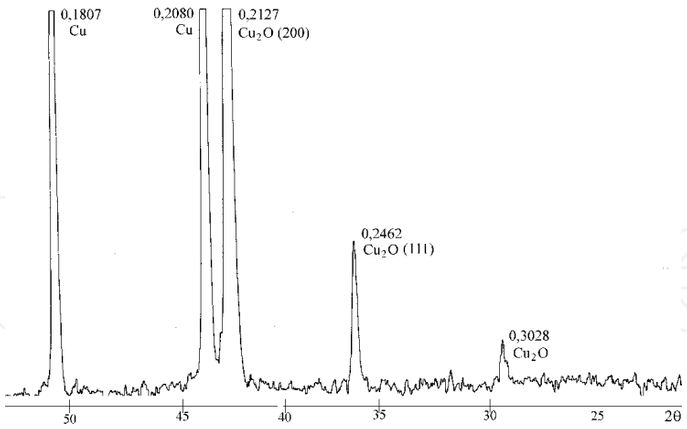

Fig. 1. X-ray diffraction spectrum of a Cu_2O film deposited on copper

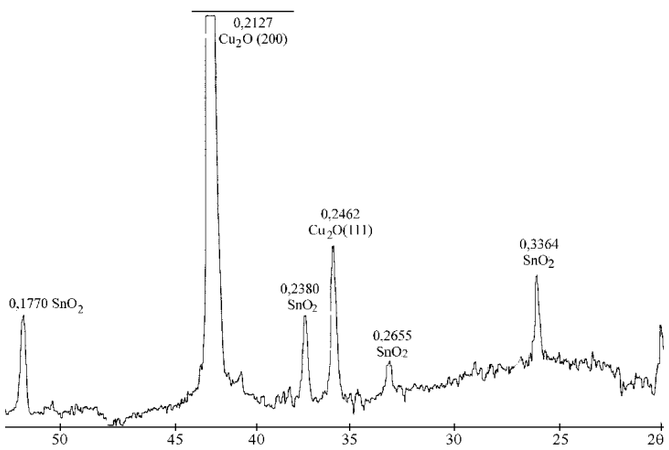

Fig. 2. X-ray diffraction spectrum of a Cu_2O film deposited on SnO_2

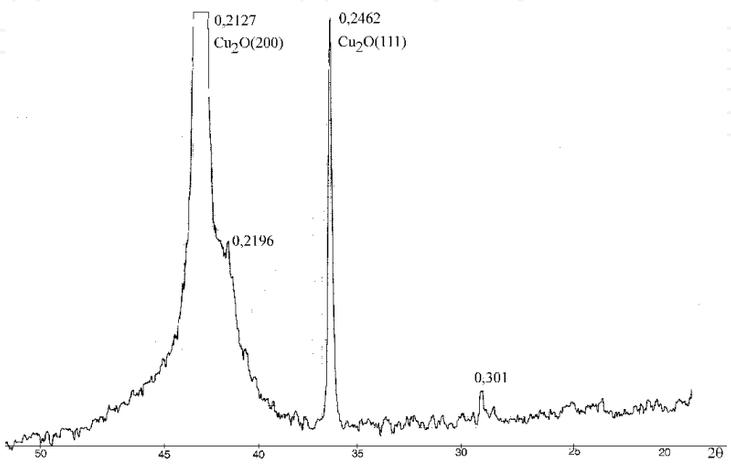

Fig. 3. X-ray diffraction spectrum of a Cu_2O film deposited on ITO

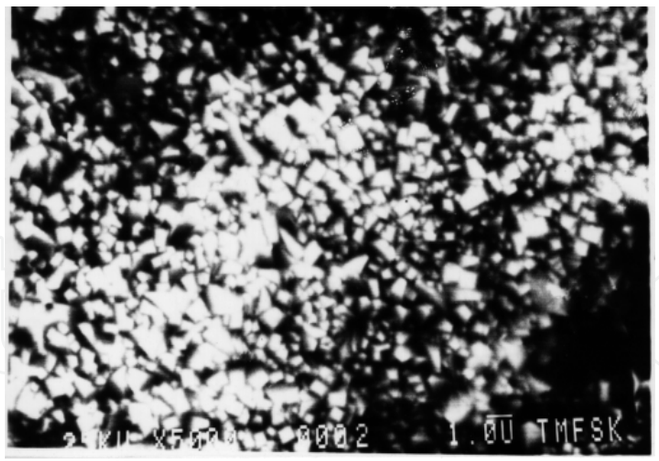

Fig. 4. Micrograph obtained from a scanning electron microscope of Cu_2O deposited on copper

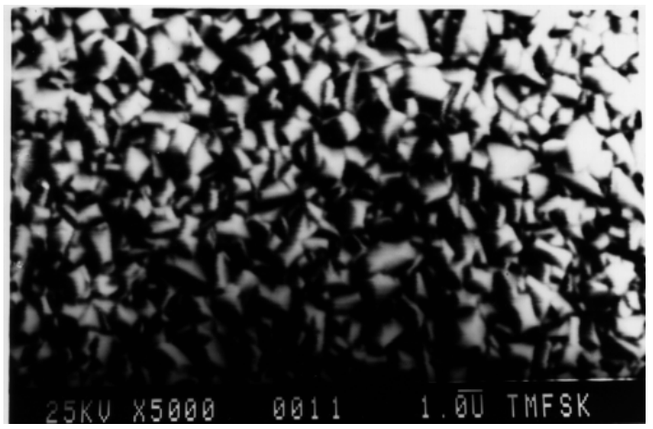

Fig. 5. Micrograph obtained from a scanning electron microscope of Cu_2O deposited on SnO

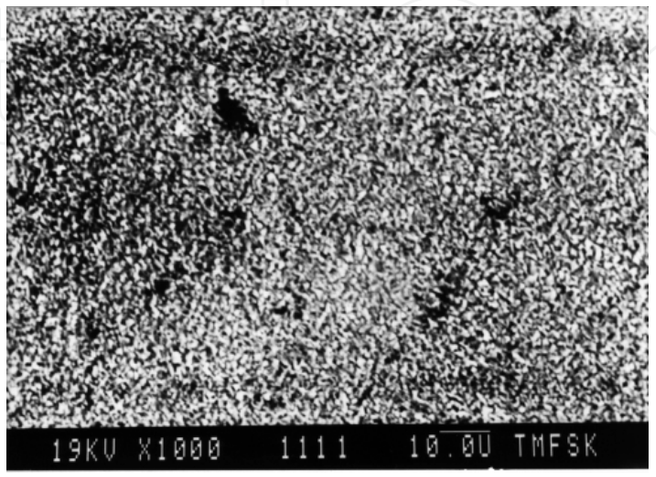

Fig. 6. Micrograph obtained from a scanning electron microscope of Cu_2O deposited on ITO

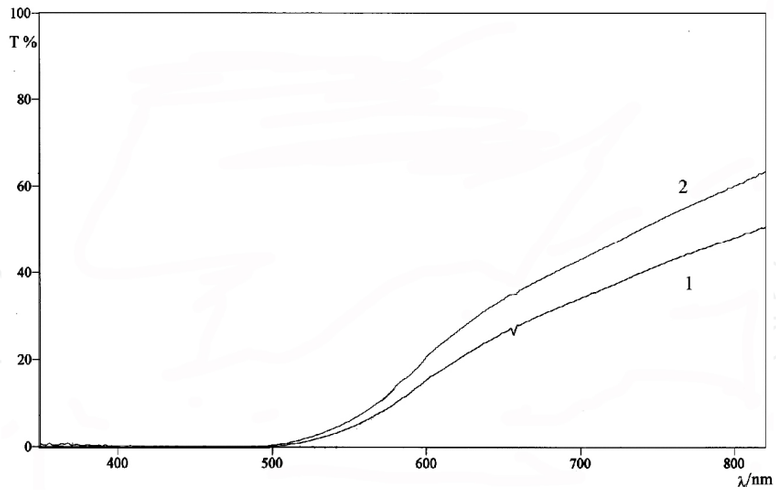

Fig. 7. Optical transmission spectrum of a 1,5 μm thick Cu_2O/SnO_2 film

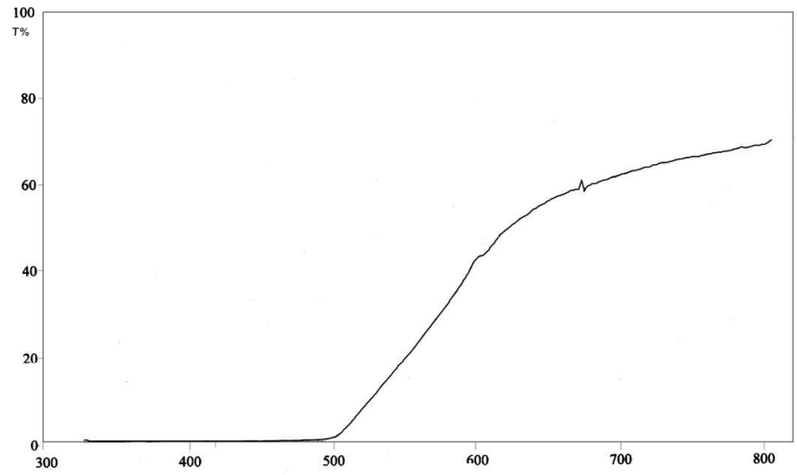

Fig. 8. Optical transmission spectrum of a 0,9 μm thick Cu_2O/ITO film

We can see that there is no difference in the spectrums. The absorption boundary is unchangeable. That means that the band gap energy is unchangeable with or without annealing. The little difference comes from different points recording, because the thickness of the film is not uniform. The transmittance spectrum of about 0,9 μm thick Cu_2O film, deposited on ITO, is presented in Fig. 8.

For determination of the optical band gap energy E_g , the method based on the relation

$$\alpha h\nu = A(h\nu - E_g)^{n/2}, \tag{1}$$

has been used, where n is a number that depends on the nature of the transition. In this case its value was found to be 1 (which corresponds to direct band to band transition) because that value of n yields the best linear graph of $(\alpha h\nu)^2$ versus $h\nu$.

The values of the absorption coefficient α were calculated from the equation

$$\alpha = \frac{A}{d}, \tag{2}$$

where d is the film's thickness determined using weighing method, and A is the absorbance determined from the values of transmittance, $T(\%)$, using the equation

$$A = \ln \frac{100}{T(\%)}. \tag{3}$$

The values of the optical absorption coefficient α ın dependence on wavelength are shown in Fig. 9 for Cu_2O/SnO_2 film and Fig. 10 for Cu_2O/ITO film

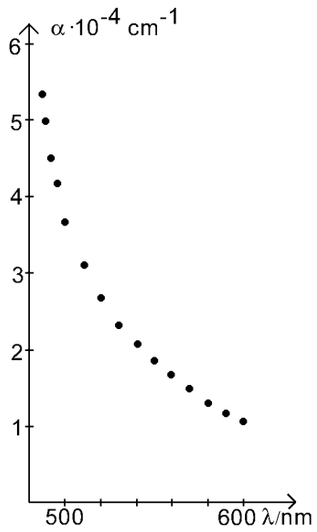

Fig. 9. Coefficient α vs wavelength λ for Cu_2O/SnO_2 film

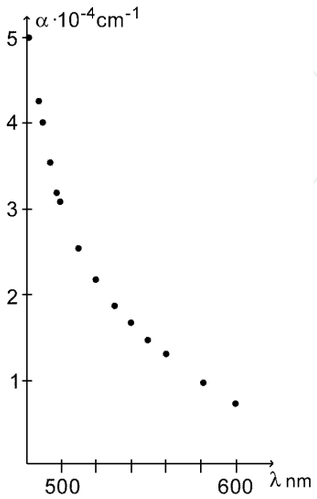

Fig. 10. Coefficient α vs wavelength λ for Cu_2O/ITO film

Fig.11 and Fig.12 show $(\alpha h\nu)^2$ versus $h\nu$ dependence for the Cu_2O/SnO_2 film and Cu_2O/ITO film corresponding. The intersection of the straight line with the $h\nu$ axis determines the optical band gap energy E_g. It was found to be 2,33 eV for Cu_2O/SnO_2 film and 2,38 eV for Cu_2O/ITO. They are higher than the value of 2 eV given in the literature and obtained for Cu_2O polycrystals. These values are in good agreement with band gaps

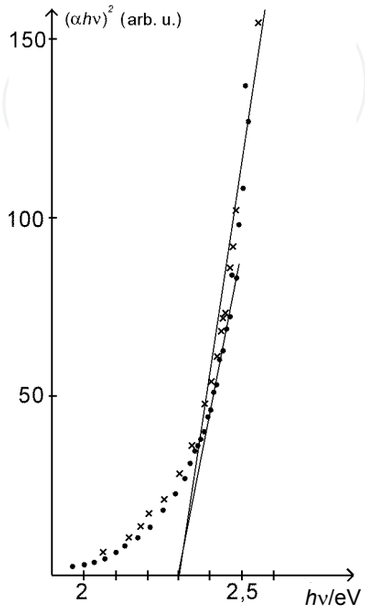

Fig. 11. Graphical determination of the optical band gap energy for Cu_2O/SnO_2 film

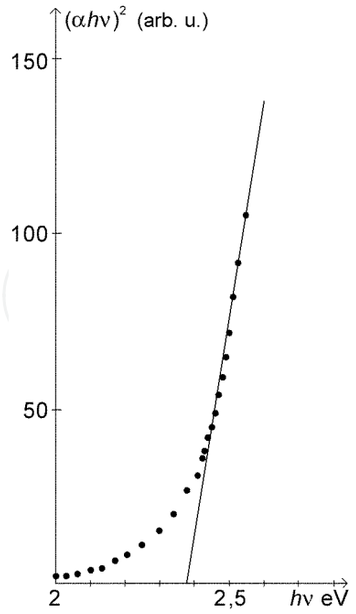

(x - before annealing; · - after annealing)

Fig. 12. Graphical determination of the optical band gap energy for Cu_2O/ITO film

determined from the spectral characteristics of the cells made with electrodeposited Cu_2O films. The value of the energy band gap of Cu_2O/ITO is little higher than the value of Cu_2O/SnO_2 film. The reason is maybe different size of the grains.
Fig.11 shows that there is no different in optical band gap energy determined from the curve plotted before annealing and from the curve plotted after annealing. Also, Fig.11 and Fig.12 show that there is no shape absorption boundary in the small energy range of the photons. Probably defects and structural irregularities are present in the films.
The optical band-gap of the films was determined using the transmitance spectrums. It was found to be 2,33 eV for Cu_2O/SnO_2 film and 2,38 eV for Cu_2O/ITO.

3. Preparation of the Cu_2O Schottky barrier solar cells

Cu_2O Schottky barrier solar cells can be fabricated in two configurations, the so called back wall and front wall structures. By vacuum evaporating a thin layer of nickel on the Cu_2O film, photovoltaic cells have been completed as back wall type cells (Fig.13), or by depositing carbon or silver paste on the rear of the Cu_2O layers, photovoltaic cells have been completed as front wall type cells (Fig.14). Nickel, carbon or silver paste are utilized to form ohmic contacts with cuprous oxide films. From the energy band diagram (Fig.15) we can see that the Cu_2O work function $\Phi_s = \chi + 1{,}7$ eV, (χ is the electron affinity of Cu_2O) (Olsen et al.,1982, Papadimitriou et al.,1990). That means that Cu_2O will make ohmic contact with metals characterized with work function higher than 4,9 eV, as are Ni, C. Gold and silver essentially form ohmic contacts. A carbon or silver back contact was chosen because of simplicity and economy of the cell preparation. The rectifying junction exists at the interface between the cooper and Cu_2O layers in the case of back wall cells. In the case of front wall cells the rectifying junction exists at the interface between the SnO_2 (ITO) and Cu_2O layers.

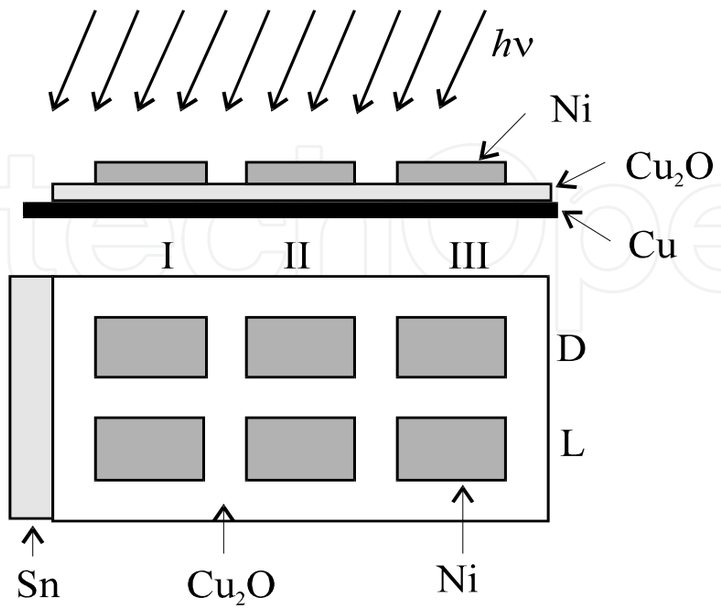

Fig. 13. Profile and face of Cu/Cu_2O back wall cell structure

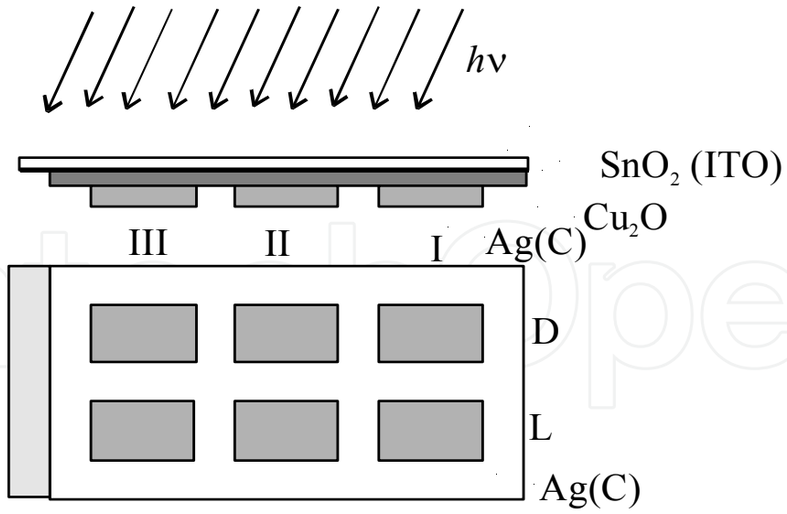

Fig. 14. Profile and rare of SnO_2 (ITO)/Cu_2O front wall cell structure

The evaporation of nickel has been made with Balzers apparatus under about 5,33 x 10^{-3} Pa pressure. The optical transmission of the nickel layer was 50% for 550nm wavelength. The total cell active area is 1.0 cm^2. Antireflectance coating or any special collection grids have not been deposited.

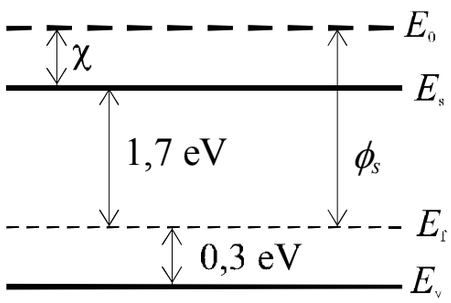

Fig. 15. Energy band diagram for Cu_2O

4. Current-voltage characteristics of the cells

The current-voltage characteristics of the best ITO/Cu_2O/C, Ni/Cu_2O/Cu and SnO_2/Cu_2O/C solar cells have been recorded in darkness and under 100 mW/cm^2 illumination, point by point. The light intensity was measured by Solar Meter Mod.776 of Dodge Products. The measurement was carried out using an artificial light source with additional glass filter, 10 mm thick to avoid heating of the cells. I-V characteristics, Fig.16, Fig.17 and Fig.18, were recorded first with periodically illumination of the source (curve ◦) to avoid the heating of the cell. After that I-V characteristics were recorded with continually illumination (curve ×). It is noted that the open circuit voltage V_{oc} and the short circuit current density I_{sc} decrease with increase in temperature. V_{oc} drops because of increase reverse current saturation with temperature because minority carriers increase with increase in temperature. I_{sc} decrease because of increase the recombination of the charges.

It should be stressed that this cells showed photovoltaic properties after heat treatment of the films for 3 hrs at 130 ^{0}C in a furnace. This possibly results in a decrease of sheet resistance value of the Cu_2O films, which was not measured, or in transformation the Cu_2O semiconductor from n to p type after heat treatment. Before heating V_{oc} and I_{sc} were about zero or negative. The serial resistance R_s and shunt resistance R_{sh} for all types of the cells were evaluated from I-V characteristics.

Cell type	R_{so} kΩ	R_s kΩ	R_{sh} kΩ
ITO/Cu_2O/C	10	1,02	76
Ni/Cu_2O/Cu	20	8,3	40
SnO_2/Cu_2O/C	14	3,3	25

Table 1. Serial and shunt resistance

The values are given in Table 1. R_{so} is evaluated from the dark characteristics (curve Δ) as dV/dI for higher values of forward applied voltage. R_{sh} is evaluated as dV/dI from the dark characteristics in reverse direction for lower values of the applied voltage (Olsen & Bohara, 1975). R_s is evaluated from the light I-V characteristics and it decreases with illumination. That means that R_s is photoresponse. The high series resistance R_s and low shunt resistance R_{sh} are one of the reasons for poor performance of the cell.
Several cell parameters were evaluated from the *I-V* characteristics. Table 2 contains the optimal current and voltage values (I_m and V_m), the open circuit voltage (V_{oc}), the short circuit current (I_{sc}) and evaluated values of the fill factor FF $\left(FF = \frac{I_m V_m}{I_{sc} V_{oc}} \right)$, the efficiency η $\left(\eta = FF \frac{I_{sc} V_{oc}}{P_{in}} \right)$ and diode factor n.

Cell type	I_m μA	V_m mV	I_{sc} μA	V_{oc} mV	FF %	η 10^{-2} %	n
ITO/Cu_2O/C	130	180	245	340	28	2,34	2,23
Ni/Cu_2O/Cu	28	120	50	270	24	0,70	2,06
SnO_2/Cu_2O/C	46	90	74	225	25	0,41	2,20

Table 2. Cell parameters

The diode factor was evaluated from the logarithmic plot of the dependence of I_{sc} versus V_{oc} which were measured for different illumination. The diode factor defined as

$$n = \frac{q}{kT} \frac{\Delta V_{oc}}{\Delta \ln I_{sc}} \tag{4}$$

is about 2 for all type of the cells.
The performances of the cells depend on the starting surface material, the type of the junction, post deposition treatment and the ohmic contact material. From the I-V characteristics, we can see that the cells are with poor performances, low fill factor FF and

very low efficiency. The high R_s and low R_{sh} (which is very far from ideally solar cell) are one of the reasons for poor performances. Because of high series resistance R_s, the values of the short circuit current density are very low. By depositing gold instead of nickel or graphite paste, the performance may be improved by decreasing of R_s.

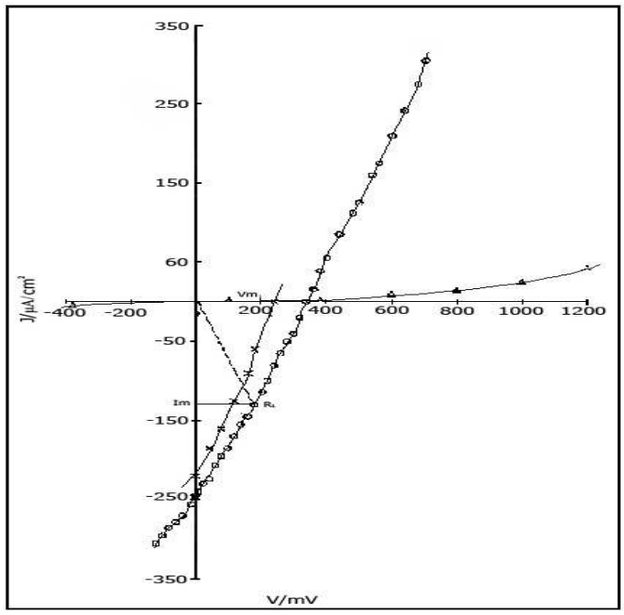

Fig. 16. I-V characteristics for ITO/Cu_2O/C solar cell ◦-periodically illumination (100 mW/cm²); ×-continually illumination(100 mW/cm²); Δ-dark characteristic

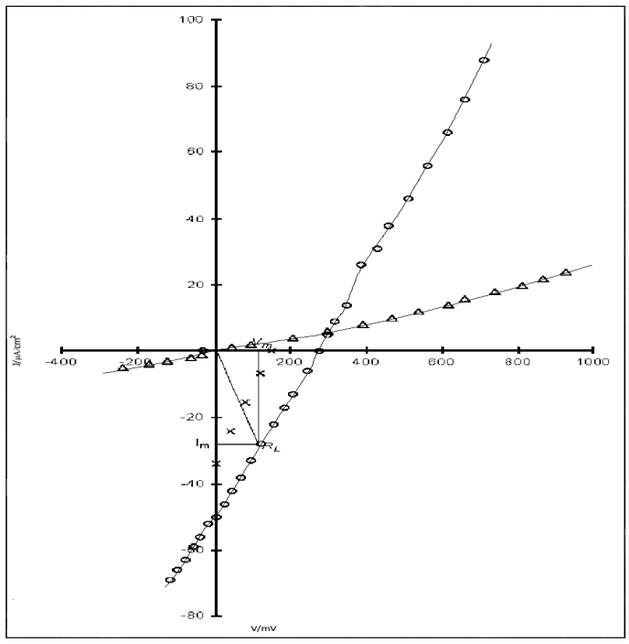

Fig. 17. I-V characteristics for Ni/Cu_2O/Cu solar cell o-periodically illumination (100 mW/cm²); ×-continually illumination(100 mW/cm²); Δ-dark characteristic

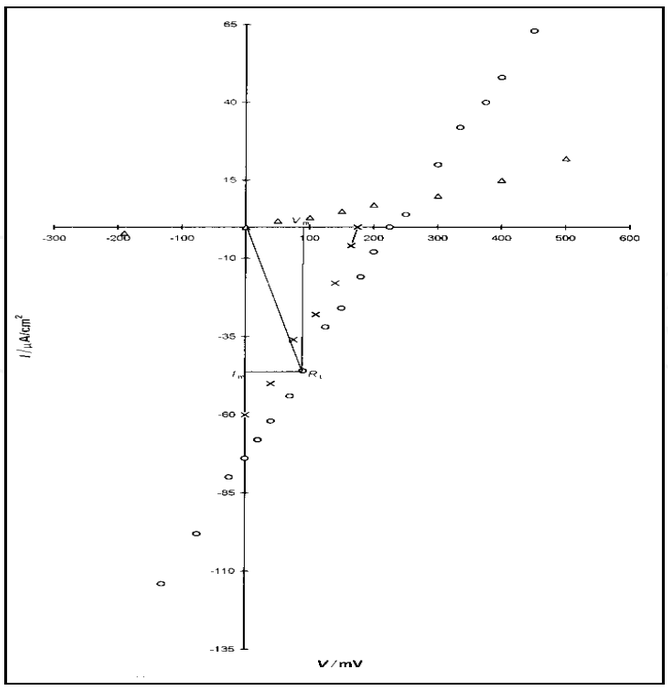

Fig. 18. I-V characteristics for $SnO_2/Cu_2O/C$ solar cell o-periodically illumination (100 mW/cm²); ×-continually illumination(100 mW/cm²); Δ-dark characteristic

5. Potential barrier height determination of the cells

Capacitance as a function of reverse bias voltage at room temperature of $Ni/Cu_2O/Cu$, SnO_2/Cu_2O/graphite and ITO/Cu_2O/graphite solar cells was measured by RCL bridge on alternating current (HP type) with built source with 1000 Hz frequency.

Results for $1/C^2$ versus reverse bias voltage for all these types of cells are shown in Fig 19, Fig 20 and Fig 21, before annealing (□), immediately after annealing (•) and after three months of annealing (×). The dependence is straight line. The intercepts of the straight line with x-axis correspond to the barrier height V_b. Cu/Cu_2O cell showed photovoltaic effect without post deposition heat treatment and their photovoltaic properties are almost unchangeable in time (fig.19). In contrast to this cell, the ITO/Cu_2O (fig.20) and SnO_2/Cu_2O (fig.21) cells no showed photovoltaic properties and no potential barrier was found to exist (Georgieva &Ristov, 2002). Before annealing, the open circuit voltage V_{oc} and the short circuit current I_{sc} were about zero.

After annealing of the films for 3 h at 130^0C, the devices exhibited good PV properties and the potential barrier excised. But this situation was not stationary. That is another essential factor in the properties of these cells indicating the possibility of chemical changes in ITO/Cu_2O and SnO_2/Cu_2O junction (Papadimitriou et al.,1981).

The values of barrier height V_b and the open circuit voltage V_{oc} upon illumination by an artificial white light source of 100 mW/cm² for all types of cells are presented in table 3. Also in this table are given their values after aging for 3 months (∗). Only Cu/Cu_2O cell has stationary values of V_b and V_{oc}. The values of barrier height V_b are great then the values of open circuit voltage V_{oc}. The great V_b gives the great $V_{oc,}$ in consent with the photovoltaic theory.

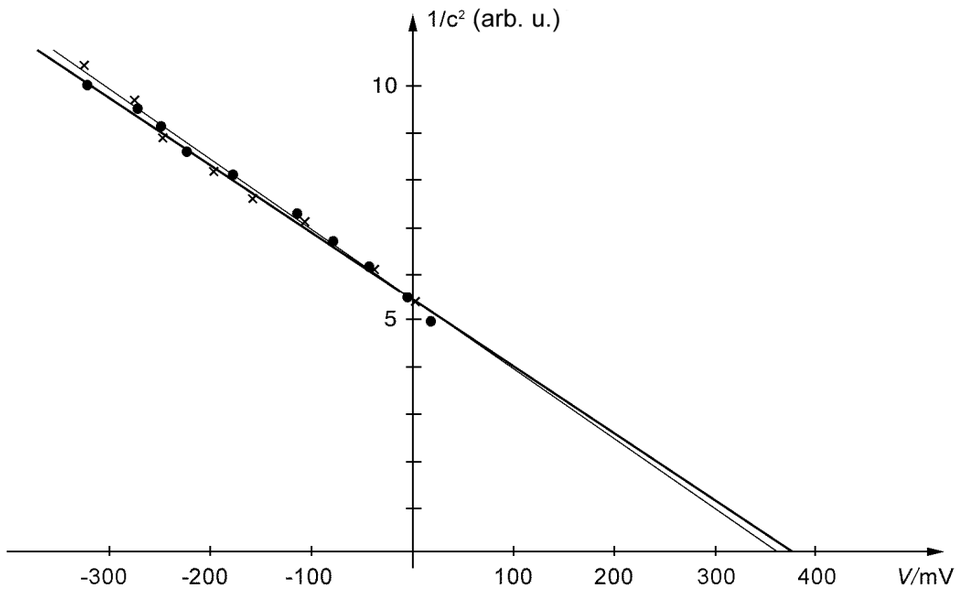

Evaluation of the barrier height, before annealing (□); after annealing (•); after 3 months of annealing (×).

Fig. 19. $1/C^2$ vs applied voltage of Cu/Cu_2O cell.

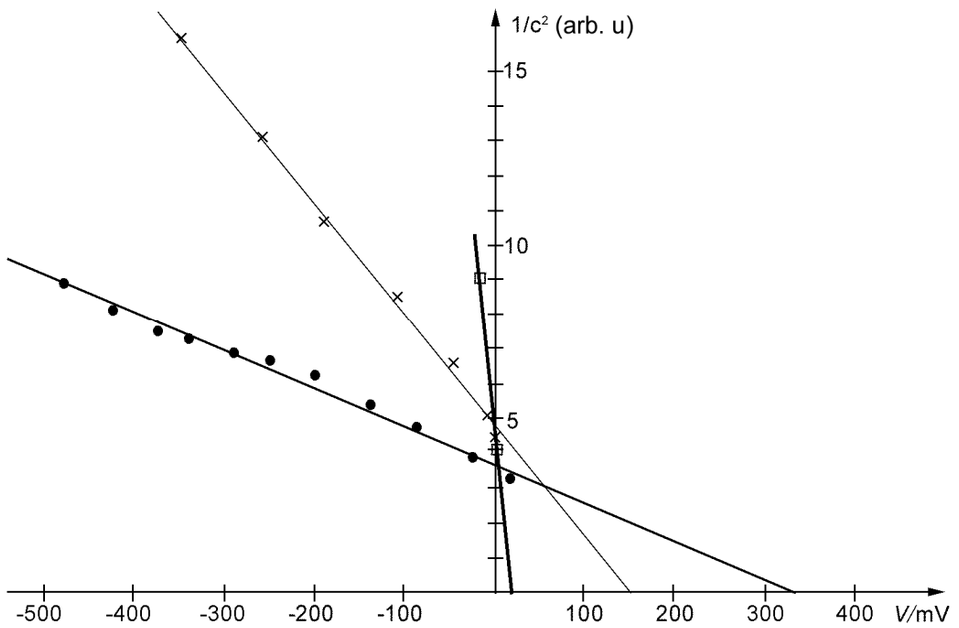

Evaluation of the barrier height, before annealing (□); after annealing (•); after 3 months of annealing (×).

Fig. 20. $1/C^2$ vs applied voltage of ITO/Cu_2O cell.

Cell type	Cu/Cu_2O	ITO/Cu_2O	SnO_2/Cu_2O	
V_b (mV)	(mV)	378	330	180
V_{oc} (mV)	310	249	118	
V_b^* (mV)	370	150	60	
V_{oc}^*(mV)	310	105	30	

Table 3. Values of barrier height V_b and open circuit voltage V_{oc} for all types of cells after annealing and after aging for 3 months (∗).

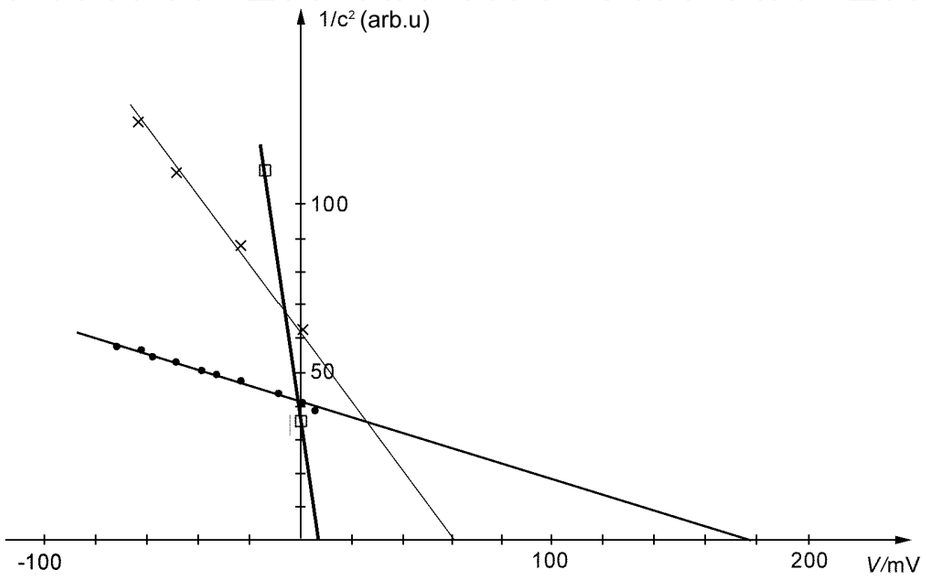

Evaluation of the barrier height, before annealing (□); after annealing (•); after 3 months of annealing (×).

Fig. 21. $1/C^2$ vs applied voltage of SnO_2/Cu_2O cell.

6. ZnO/Cu_2O heterojunction solar cells

Until now, we have made Schottky barrier solar cells. As we could not improve their efficiency and their stability, we decided to make heterojunction p-n solar cells based on a p-type Cu_2O thin films. We selected ZnO as an n-type semiconductor. ZnO is a transparent oxide that is widely used in many different applications, including thin film solar cells. The p-n junction was fabricated by potentiostatic deposition of the ZnO layer onto SnO_2 conducting glass with a sheet resistance of 14 Ω/ and potentiostatic deposition of Cu_2O onto ZnO, Fig.22.

6.1 Electrochemical depositing of ZnO

ZnO/Cu_2O heterojunction solar cells were made by consecutive cathodic electrodeposition of ZnO and Cu_2O onto tin oxide covered glass substrates. Zinc oxide (ZnO) was cathodically deposited on a conductive glass substrate covered with SnO_2 as cathode by a potentiostatic method (Dalchiele et al.,2001, Izaki et al.,1998, Ng-Cheng-Chin et al.,1998). Conducting glass slides coated with SnO_2 films are commercial samples. The electrolysis takes place in a

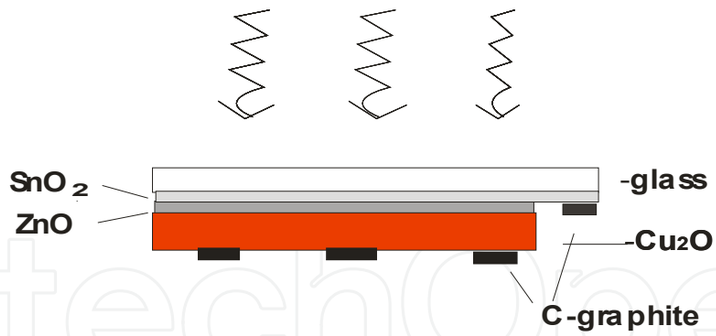

Fig. 22. Profil of ZnO/Cu_2O hetrojunction solar cells

simple aqueous 0,1M zinc nitrate [Zn $(NO_3)_2$] solution with pH about 6, maintained at 70^0C temperature. The cathodic process possibly can be described by the following reaction equations (Izaki & Omi, 1992):

$$Zn(NO_3)_2 \rightarrow Zn^{2+} + 2NO_3^-$$

$$NO_3^- + H_2O + 2e^- \rightarrow NO_2 + 2OH^-$$

$$Zn^{2+} + 2OH^- \rightarrow Zn(OH)_2 \rightarrow ZnO + H_2O \quad (5)$$

ZnO films were electrochemically grown at constant potential of 0.8 V between the anode and cathode. For a fixed value of the potential, a current density decreased with increasing the film thickness. The deposition time was varying from 10 min to 30 min. Deposited films were rinsed thoroughly in distilled water and allowed to dry in air at room temperature. The anode was zinc of 99.99% purity.

The deposition conditions of the thin films of Cu_2O have been described in 2.1.1. The deposition potential is pH sensitive. It suggests, also and it has already been reported that the Cu_2O layer was formed by the following reaction:

$$2Cu^{2+} + 2e^- + 2OH^- \rightarrow Cu_2O + H_2O, \quad (6)$$

even this reaction does not explain the large pH dependence of deposition potential (Izaki et al. 2007, Wang & Tao, 2007). The present study was conducted, in a first instance, on undoped zinc oxide films and cuprous (I) oxide films. The structure of the films was studied by X-ray diffraction measurements using monochromatic Cu K_α radiation with a wavelength of 0,154 nm operated at 35 kV and 24 mA. Morphology and grain size was determined through micrographs on a JEOL JSM 6460 LV scanning electron microscope.

Figure 23 shows the X-ray diffraction patterns of ZnO film prepared at 0.8 V potential for 10 min. The Bragg angle of 2θ was varied between 20^0 and 70^0. It can be seen that the film has crystalline structure. XRD peaks corresponding to ZnO (signed as C) and the substrate material SnO_2 (signed as K) were determined with JCPDS patterns. The XRD spectrum indicates a strong ZnO peak with a (0002) or (1011) preferential orientation.

Figure 24 shows a scanning electron micrograph of undoped electrodeposited ZnO film.The photograph shows small rounded grains. It is difficult to determine the grain size from the micrograph. But using Scherrer's equation ($D = \frac{0,9\lambda}{\beta \cos\theta}$), the apparent crystallite size of ZnO is about 20nm, which means that it is nanostructured film

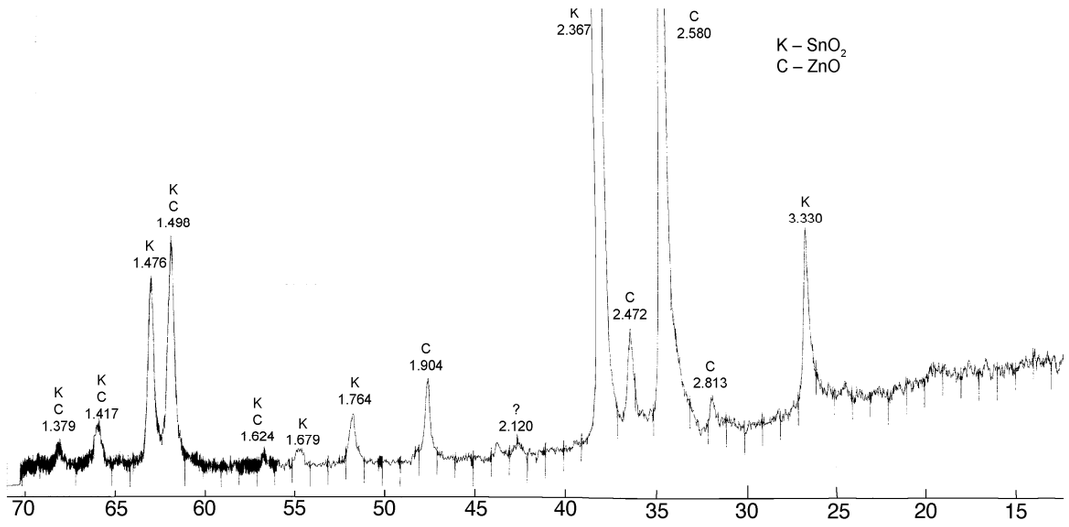

Fig. 23. X-ray diffraction spectrum of undoped electrodeposited ZnO film at 65^0C

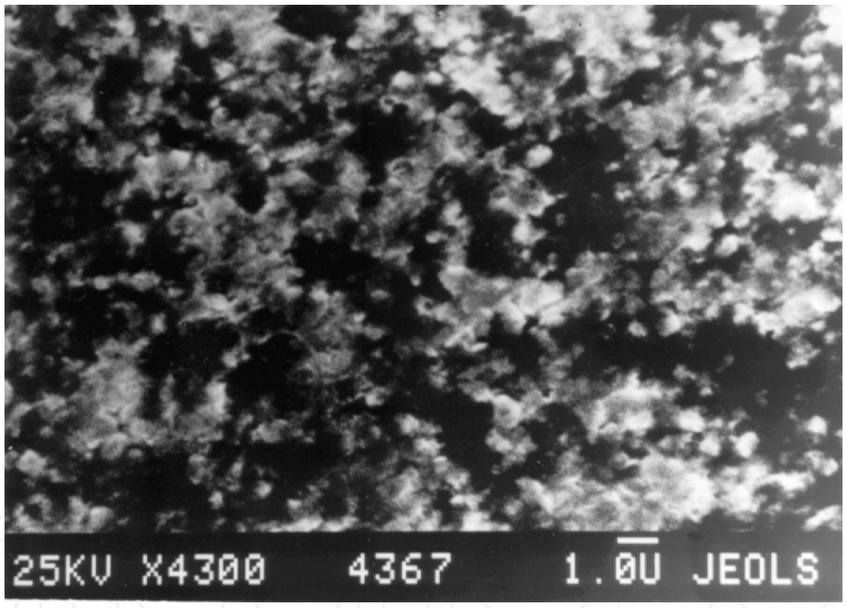

Fig. 24. SEM micrograph of undoped electrodeposited pure ZnO

Thin films of ZnO grown by electrochemical deposition technique on SnO_2/glass substrate are optically transparent in a visible spectral region, extending to 300 nm wavelength.

The transmission is relatively low (~ 50%) in the blue region (400–450 nm) Fig.25. The transmission maximum is about 60–70% through the red light region. Probably defects and structural irregularities are presented in the films, indicating low transmission.

Assuming an absorption coefficient α corresponding to a direct band to band transition and making a plot of $(\alpha h\nu)^2$ versus energy $h\nu$, the optical band gap energy Eg was determined through a linear fit. It was found to be 3.4 eV , which corresponds to the documented room temperature value of 3.2 to 3.4 eV.

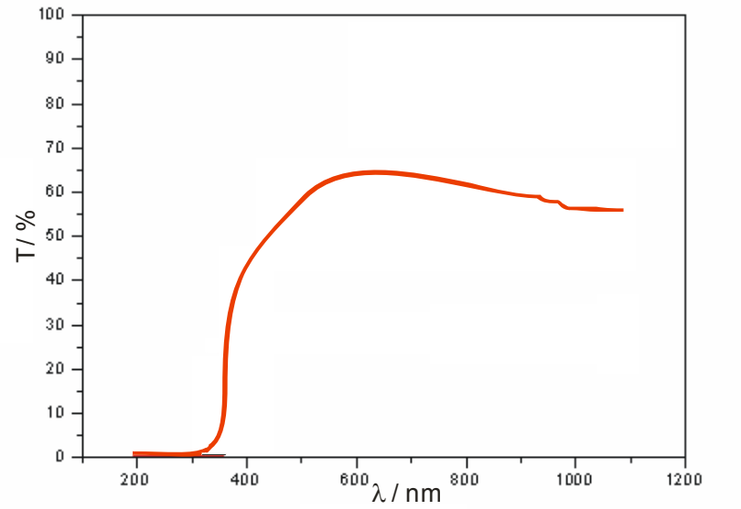

Fig. 25. Optical transmission spectrum of ZnO film

6.2 Some characteristic of the cells

To complete $Cu_2O/ZnO/SnO_2$ heterojunction as solar cell, thin layer of carbon paste or carbon spray was deposited on the rear of the Cu_2O. Front wall cells were formed. A carbon back contact was chosen because of simplicity and economy of the cell preparation and because the cells with carbon give high values of the short circuit current density despite the evaporated layer of nickel. The total cell active area was 1 cm². Antireflectance coating or any special collection grids have not been deposited. The best values of the open circuit voltage $V_{o\,c}$= 330 mV and the short circuit current density I_{sc} = 400 μm/cm² were obtained by depositing carbon paste and illumination of 100 mW/cm². The V_{oc} increases as logarithmic function with solar radiation, ($Voc = \frac{kT}{e}\ln\left(\frac{I_{sc}}{I_0}+1\right)$). The *Isc* increases linear with solar radiation, (Fig.26).

Our investigations show that the ZnO layer improves the stability of the cells. That results in a device with better performances despite of the Schhotky barrier solar cells (Cu_2O/SnO_2). First, the cells show photovoltaic properties without annealing, because potential barrier was formed without annealing. The barrier fell for a few days which result in decreasing the open circuit voltage despite the values of V_{oc} for just made cells. It decreases from 330 mV to 240 mV. But after that the values of V_{oc} keep stabilized, because of stabilized barrier potential. It wasn't case with Schotkky barrier solar cells, because barrier potential height decreases with aging. In ZnO/Cu_2O cells, thermal equilibrium exists. The V_{oc} decreases and I_{sc} increases with increasing the temperature, that is characteristic for the real solar cell. It could be seen from the current-voltage (*I-V*) characteristic in incident light of 50mW/cm², Fig.27.

Barrier potential height was determined for one device from capacitance measurement as a function of reverse bias voltage at room temperature. Capacitance dependence of reverse bias voltage at room temperature was measured by RCL bridge on alternating current (HP type) with bilt source with 1000 Hz frequency. Results for ($1/C^2$) versus voltage are shown in Figure 28. The Cu_2O/SnO_2 cells without the ZnO layer show a lower V_{oc}. The improvement in V_{oc} could be due to the increase of the barrier height using ZnO layer as n-type semiconductor.

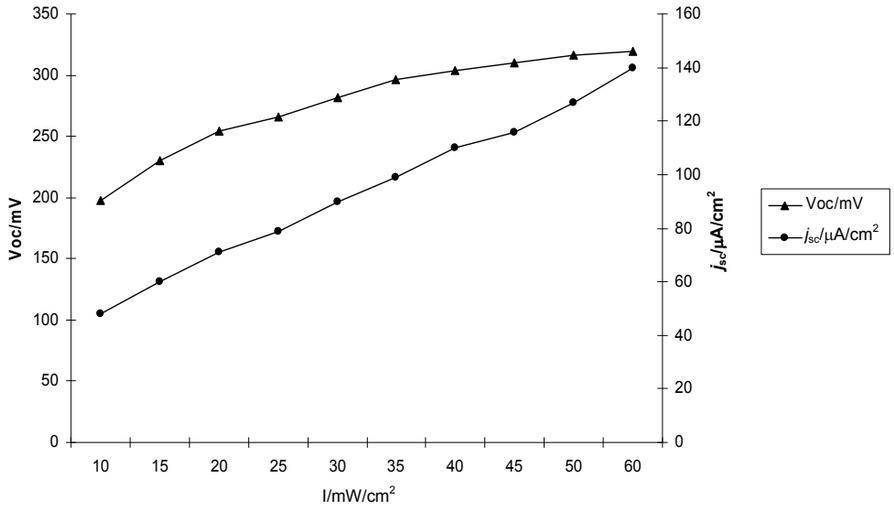

Fig. 26. Dependence of the V_{oc} and I_{sc} vs. solar irradiation

The values of barrier height V_b and the open circuit voltage V_{oc} upon illumination of 100 mW/cm² for just made cell and the cell after few days are presented in table 4. Also in this table are given their values after few days of depositing. The values of the barrier height are great than the values of open circuit voltage V_{oc}. The grate V_b gives the great V_{oc}, that correspondent to the photovoltaic theory.

$Cu_2O/ZnO/SnO_2$ cell	V_b(mV)	V_{oc}(mV)
just made	368	330
after few days	276	240

Table 4. Values of barrier height V_b and open circuit voltage V_{oc} for just made cell and after few days.

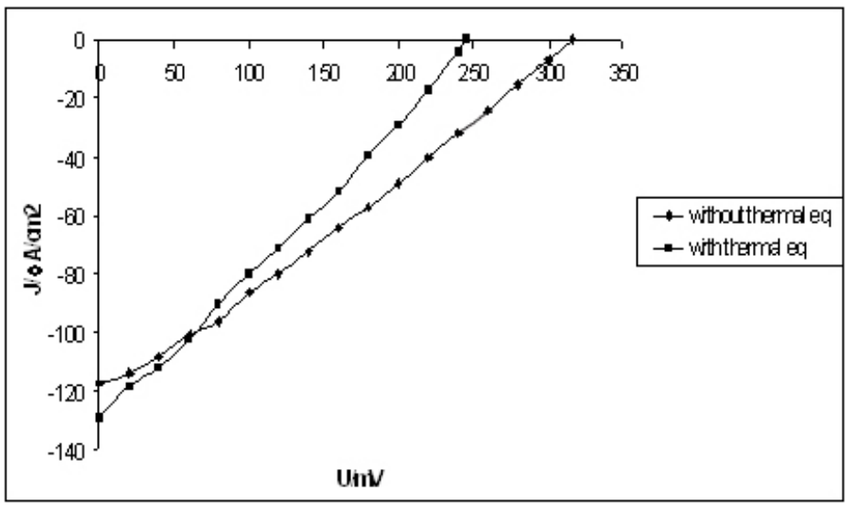

Fig. 27. Volt-current characteristics of the $Cu_2O/ZnO/SnO_2$ solar cell upon 50mW/cm² Illumination

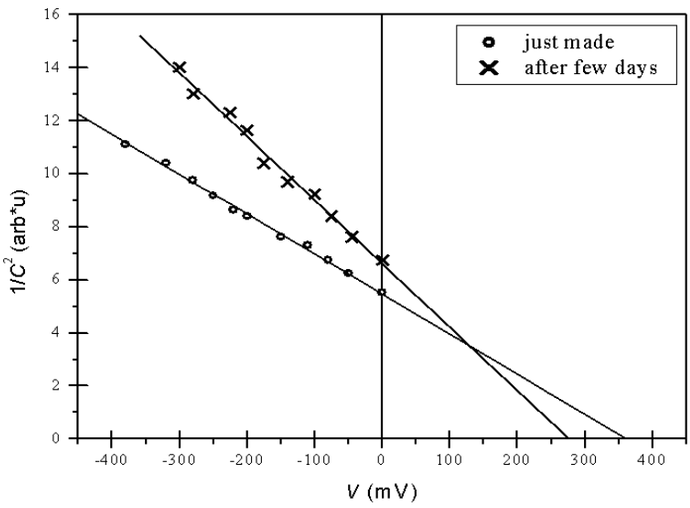

Fig. 28. $1/C^2$ vs applied voltage of $Cu_2O/ZnO/SnO_2$ cell

The values Voc=316 mV, Isc=0,117 mA/cm², fill factor =0,277, upon 50mW/cm² illumination are compared with the values: Voc=190 mV, Isc=2,08 mA/cm², fill factor = 0,295; upon 120mW**/cm²** illumination (Katayama et al. 2004) made with electrochemical deposition technique. Maybe doping of the ZnO films with In, Ga and Al (Machado et al., 2005, Kemell et al., 2003) will decrease the resistivity and increase the electro conductivity of the films, consequently and the short circuit current density of the cells.

7. Conclusion

The performance of the Cu_2O Schottky barrier solar cells are found to be dependent on the starting surface material, the type of the junction, post deposition treatment and the ohmic contact material. Better solar cells have been made using an heterojunction between Cu_2O and n-type TCO of ZnO. It is a suitable partner since it has a fairly low work function. Our investigation shows that the ZnO layer improves the stability of the cells. That results in a device with better performances despite of the Schhotky barrier solar cells (Cu_2O/SnO_2). First, the cells show photovoltaic properties without annealing, because potential barrier was formed without annealing. To improve the quality of the cells, consequently to improve the efficiency of the cells, it has to work on improving the quality of ZnO and Cu_2O films, because they have very high resistivity, a factor which limits the cells performances. Doping of the ZnO films with In, Ga and Al will decrease the resistivity of the deposited films and increase their electroconductivity. SEM micrographs show that same defects are present in the films which act as recombination centers. Behind the ohmic contact, maybe one of the reason for low photocurrent is just recombination of the carriers and decreasing of the hole cocentracion with the time. The transmittivity in a visible region have to increase. Also, it is necessary to improve the ohmic contact, consequently to increase the short circuit current density (*Isc*). For further improvement of the performances of the cells maybe inserting of a buffer layer at the heterojunction between Cu_2O and ZnO films will improve the performance of the cells by eliminating the mismatch defects which act as recombination centers. Also it will be protection of reduction processes that maybe exists between ZnO and Cu_2O.

Even low efficiency it may be acceptable in countries where the other alternative energy sources are much more expensive.

8. Acknowledgment

Part of this work has been performed within the EC funded RISE project (FP6-INCO-509161). The authors want to thank the EC for partially funding this project.

9. References

Dalchiele E.A., Giorgi P.,.Marotti R.E, at all. Electrodeposition of ZnO thin films on n-Si(100), *Solar Energy Materials &Solar Cells* 70 (2001) 245-254

GeorgievaV. Ristov M. (2002) Electrodeposited cuprous oxide on indium tin oxide for solar applications, *Solar Energy Materials & Solar Cells* 73, p 67-73

Izaki M., Omi T,J. (1992).,*Electrochem.Soc.*1392014

Izaki M, Ishizaki H., Ashida A. at all. (1998), *J.Japan Inst.Metals*, Vol. 62,No.11pp.1063-1068

Izaki M., Shinagawa T., Mizuno K., Ida Y., Inaba M., and Tasaka A., (2007) Electrochemically constructed p-Cu_2O/n-ZnO heterojunction diode for photovoltaic device *J.Phys.D:Appl.Phys*.40 3326-3329.

Jayanetti J.K.D., Dharmadasa I.M, (1996), *Solar Energ.Mat.andSolar Cells* 44 251-260

Katayama J., Ito K. Matsuoka M. and Tamaki J., (2004) Performance of Cu_2O/ZnO solar cells prepared by two-step electrodeposition *Journal of Applied Electrochemistry*, 34: 687-692,

Kemell M., Dartigues F., Ritala M., Leskela M, (2003) Electrochemical preparation of In and Al doped Zno thin films for $CuInSe_2$ solar cells, *Thin Solid Films* 434 20-23

Machado G., Guerra D.N., Leinen D., Ramos-Barrado J.R. Marotti R.E., Dalchiele E.A., (2005), Idium doped zinc oxide thin films obtained by electrodeposition ,*Thin Solid Films* 490 124-131

Minami T.,.Tanaka H, Shimakawa T., Miyata T., Sato H., (2004) High-Efficiency Oxide Heterojunction Solar cells Using Cu_2O Sheets *Jap.J.Appl.Phys*.,43, p.917-919

Mukhopadhyay A.K.,.Chakraborty A.K, Chattarjae A.P. and.Lahriri S.K, (1992), *Thin Solid Films*, 209, 92-96

Olsen L.C., Bohara R.C., Urie M.W., (1979) *Appl.Phys.Lett,* 34, p. 47

Olsen L.C., Addis F.W. and Miller W., (1982-1983), *Solar Cells*, 7 247-249

Papadimitriou L., Economu N.A and Trivich, (1981), *Solar Cells*, 3 73

Papadimitriou L., Valassiades O. and Kipridou A., (1990), *Proceeding,* 20th ICPS, Thessaloniki, 415-418

Ng-Cheng-Chin F., Roslin M.,.Gu Z.H and Fahidy T.Z., (1998) *J.Phys.D.Appl.Phys*.31 L71-L7

Rai B.P., (1988) Cu_2O Solar Cells *Sol. Cells* 25 p.265.

Rakhshani A.E (1986) Preparation, characteristics and photovoltaic properties of cuprous oxide-A review *Solid-State Electronics* Vol. 29.No.1. pp.7-17.

Rakhshani A.E., Jassar A.A.Al and.Varghese J. (1987) Electrodeposition and characterization of cuprous oxide *Thin Solid Films*, 148,pp.191-201

Rakhshani A.E.and Varghese J., (1987) Galvanostatic deposition of thin films of cuprous oxide *Solar Energy Materials*, 15,23,

Rakhshani A.E., Makdisi Y. and Mathew X., (1996), *Thin Solid Films*, 288, 69-75

Stareck, U.S. Patents 2, 081, 121 *Decorating Metals*, 1937

Wang L. and Tao M. (2007) Fabrication and Characterization of p-n Homojunctions in Cuprous Oxide by Electrochemical Deposition, *Electrochemical and Solid-State Letters*, 10 (9) H248-H250

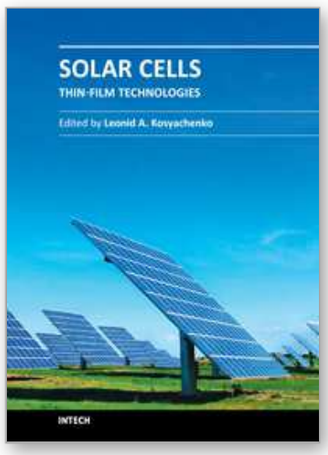

Solar Cells - Thin-Film Technologies

Edited by Prof. Leonid A. Kosyachenko

ISBN 978-953-307-570-9
Hard cover, 456 pages
Publisher InTech
Published online 02, November, 2011
Published in print edition November, 2011

The first book of this four-volume edition is dedicated to one of the most promising areas of photovoltaics, which has already reached a large-scale production of the second-generation thin-film solar modules and has resulted in building the powerful solar plants in several countries around the world. Thin-film technologies using direct-gap semiconductors such as CIGS and CdTe offer the lowest manufacturing costs and are becoming more prevalent in the industry allowing to improve manufacturability of the production at significantly larger scales than for wafer or ribbon Si modules. It is only a matter of time before thin films like CIGS and CdTe will replace wafer-based silicon solar cells as the dominant photovoltaic technology. Photoelectric efficiency of thin-film solar modules is still far from the theoretical limit. The scientific and technological problems of increasing this key parameter of the solar cell are discussed in several chapters of this volume.

INTECH
open science | open minds

InTech Europe
University Campus STeP Ri
Slavka Krautzeka 83/A
51000 Rijeka, Croatia
Phone: +385 (51) 770 447
Fax: +385 (51) 686 166
www.intechopen.com

InTech China
Unit 405, Office Block, Hotel Equatorial Shanghai
No.65, Yan An Road (West), Shanghai, 200040, China
中国上海市延安西路65号上海国际贵都大饭店办公楼405单元
Phone: +86-21-62489820
Fax: +86-21-62489821

IntechOpen